

## Motion of microgel particles under an external electric field

This article has been downloaded from IOPscience. Please scroll down to see the full text article.

2000 J. Phys.: Condens. Matter 12 3605

(<http://iopscience.iop.org/0953-8984/12/15/309>)

View [the table of contents for this issue](#), or go to the [journal homepage](#) for more

Download details:

IP Address: 171.66.16.221

The article was downloaded on 16/05/2010 at 04:48

Please note that [terms and conditions apply](#).

## Motion of microgel particles under an external electric field \*

A Fernández-Nieves†, A Fernández-Barbero†, F J de las Nieves†§ and  
B Vincent‡

† Group of Complex Fluids Physics, Department of Applied Physics, University of Almería,  
04120 Almería, Spain

‡ School of Chemistry, Cantock's Close, University of Bristol, Bristol BS8 1TS, UK

Received 16 August 1999, in final form 2 November 1999

**Abstract.** The influence of the swelling of charged microgel particles on their motion under an external electric field has been studied. The selected experimental observable was the electrophoretic mobility of the particles, which was measured as a function of the pH since its value controls the electrical charge of the particles. The mobility–pH curve presents a maximum and a minimum as a consequence of the competition between charge-density and friction coefficient variations during swelling. Ohshima's theory for polyelectrolyte-coated particles was employed, describing qualitatively the experimental results. Quantitative discrepancies suggest that charge renormalization should be considered.

### 1. Introduction

Polyelectrolyte macrogels are three-dimensional charged polymer networks capable of undergoing large swelling transitions. This phase change is controlled by competing elastic, solvency and ionic contributions [1], the last mentioned being sensitive to the degree of ionization of the network groups, and thus to the pH and ionic strength.

Microgels are gel particles in the colloidal size range. The swelling behaviour resembles that of macrogels in many respects but, because of their size and charge distribution, additional phenomena may be encountered. Microgels are finding a large number of applications, in fields as diverse as medicine and biology [2, 3], industry [4, 5] and environmental clean-up [6].

In the present paper, we describe the influence of microgel swelling on the electrophoretic mobility. The pH was selected as the external variable triggering the swelling, since the microgel network used contained ionizable groups. The mobility exhibits a maximum and a minimum as a function of pH, which is explained as a competition between variations in the charge density and friction coefficient of the polymer network. The theoretical approach is based on Ohshima's theory for the electrophoresis of polyelectrolyte-coated particles [7]. This approach requires the knowledge of certain particle characteristics, such as the charge distribution. The microgel surface and bulk charges have been determined in a previous work [8]. Internal structure modifications within the particle as it swells are described in terms of changes in the friction coefficient, using the expression proposed by Cohen Stuart *et al* [9]. Good, qualitative agreement between theory and experiment has been found. However, quantitative discrepancies suggest that some form of charge renormalization, probably in terms of an ion condensation effect, needs to be considered.

\* Originally presented as a poster at the Fourth EPS Liquid Matter Conference, Granada, Spain, 3–7 July 1999.

§ Author to whom any correspondence should be addressed.

## 2. Electrophoretic mobility of a polyelectrolyte-coated particle

The velocity  $\vec{U}$  of a charged colloidal particle moving in the presence of a weak electric field  $\vec{E}$  is linearly related to the strength of the applied field [10]:

$$\vec{U} = \mu \vec{E} \quad (1)$$

where  $\mu$  is the electrophoretic mobility of the particle. This coefficient contains information not only on the particle net charge but also on the distribution of the ions in the vicinity of the particle. In the case of microgel particles, ions may distribute within the particle network, modifying the inner net charge.

Ohshima [7] has presented a general theoretical study of the electrophoresis of polyelectrolyte-coated particles. One of the achievements of this theory has been the amalgamation of theories for rigid spheres with those developed for spherical polyelectrolytes.

The fluid motion is described by the Navier–Stokes equation, neglecting inertial terms (low Reynolds number). For steady and incompressible flow, the following equations apply:

$$\eta \vec{\nabla} \times \vec{\nabla} \times \vec{u}(\vec{r}) + \vec{\nabla} p(\vec{r}) + \rho_{el} \vec{\nabla} \psi(\vec{r}) + \vec{\gamma} \cdot \vec{u}(\vec{r}) = 0 \quad a < r < b \quad (2)$$

$$\eta \vec{\nabla} \times \vec{\nabla} \times \vec{u}(\vec{r}) + \vec{\nabla} p(\vec{r}) + \rho_{el} \vec{\nabla} \psi(\vec{r}) = 0 \quad r > b \quad (3)$$

$$\vec{\nabla} \cdot \vec{u}(\vec{r}) = 0 \quad (4)$$

where  $a$  and  $b$  are the particle core and outer periphery radii, respectively;  $\vec{u}(\vec{r})$  is the fluid velocity;  $p(\vec{r})$  is the pressure and  $\rho_{el}$  the charge density associated with the mobile ions.  $\psi(\vec{r})$  is the electric potential and  $\vec{\gamma}$  the friction tensor describing the friction between the polyelectrolyte layer and the liquid. The frictional force is only relevant within the polyelectrolyte region (equation (2)). Outside this zone, there is no frictional term (equation (3)). Equation (4) is the continuity equation, expressing mass conservation for incompressible flow.

The ionic flow velocity  $\vec{v}_i(\vec{r})$ , for the  $i$ th ionic species, is given in equation (5); the ions move because of the motion of the fluid and due to gradients in the chemical potential  $\mu_i(\vec{r})$  (equation (6));  $\lambda_i$ ,  $z_i$  and  $n_i(\vec{r})$  are the drag coefficient, valency and number density of the  $i$ th ionic species, respectively; equation (7) expresses the conservation of mass for the  $i$ th ionic species:

$$\vec{v}_i = \vec{u} + \frac{1}{\lambda_i} \vec{\nabla} \mu_i(\vec{r}) \quad (5)$$

$$\mu_i = \mu_i^\infty + z_i e \psi(\vec{r}) + kT \ln n_i(\vec{r}) \quad (6)$$

$$\vec{\nabla} \cdot (n_i(\vec{r}) \vec{v}_i(\vec{r})) = 0. \quad (7)$$

The electrostatics of the system is expressed through the Poisson equation, both inside and outside the polyelectrolyte layer:

$$\nabla^2 \psi(\vec{r}) = \frac{\rho_{el}}{\epsilon_0 \epsilon_r} + \frac{\rho_{fix}}{\epsilon_0 \epsilon_r} \quad a < r < b \quad (8)$$

$$\nabla^2 \psi(\vec{r}) = \frac{\rho_{el}}{\epsilon_0 \epsilon_r} \quad r > b \quad (9)$$

where the charge densities due to the mobile ions and fixed polyelectrolyte charges are expressed as:

$$\rho_{el} = \sum z_i e n_i(\vec{r}) \quad (10)$$

$$\rho_{fix}(\vec{r}) = \rho_{fix}(r) = Ze N_a \rho(r) \quad (11)$$

The difference between equations (8) and (9) is the additional term in equation (8), which is associated with the presence of fixed charges in the shell region. Equation (11) assumes that this charge density is distributed with spherical symmetry.  $Z$  is the valence of the fixed groups in the shell and  $N_a$  the Avogadro number.  $\rho$  is expressed in moles per unit volume.

In the limit  $a \rightarrow 0$ , the particle core vanishes, so the particle becomes a spherical polyelectrolyte, i.e. a porous charged sphere. In this limit, the general expression for the electrophoretic mobility reduces to the equation [7]:

$$\begin{aligned} \mu = & \frac{2}{b}h(b) + \frac{b^2}{9} \int_b^\infty \left(1 - \frac{3r^2}{b^2} + \frac{2r^3}{b^3}\right) G(r) \, dr \\ & - \frac{2}{3\lambda^2} \int_0^b \left(\frac{r^3}{b^3} - \frac{\cosh(\lambda r) - [\sinh(\lambda r)]/\lambda r}{\cosh(\lambda b) - [\sinh(\lambda b)]/\lambda b}\right) G(r) \, dr \\ & + \frac{2}{3\lambda^2} \left(1 - \frac{b\lambda}{3} \frac{\sinh(\lambda b)}{\cosh(\lambda b) - [\sinh(\lambda b)]/\lambda b}\right) \int_b^\infty \left(1 - \frac{r^3}{b^3}\right) G(r) \, dr \end{aligned} \quad (12)$$

where

$$\lambda = \left(\frac{\gamma}{\eta}\right)^{1/2} \quad (13)$$

and

$$h(b) = \frac{3}{2\eta\lambda^2 b^2} \int_0^b \rho_{fix} r^2 \, dr. \quad (14)$$

The radial function  $G(r)$  and the constant  $h(b)$  contain the electrical parameters for the particle. For low potentials and homogeneously distributed charge, i.e.  $\rho_{fix}(r) = \rho_{fix}$ ,  $G(r)$  takes the following, simple form:

$$G(r) = \frac{\epsilon_0 \epsilon_r \kappa^2}{\eta} \frac{d}{dr} \psi^{(0)} \quad (15)$$

in which  $\psi^{(0)}$  is the electric potential at equilibrium—that is, in the absence of the external electric field.  $\kappa$  is the inverse of the Debye length:

$$\kappa = \left(\frac{1}{\epsilon_0 \epsilon_r kT} \sum_i z_i^2 e^2 n_i^{bulk}\right)^{1/2}. \quad (16)$$

### 3. Model for the particle charge distribution

In order to solve equation (12), a specific model for the charge distribution within the particle must be assumed. The experimental system under consideration is a positively charged microgel with surface and volume charges, undergoing a swelling transition at  $\text{pH} = \text{pH}_t$  [8, 11] (see section 4 for particle details). Above this  $\text{pH}$  value, the particle is in its unswollen state, and thus only the surface charge is relevant. Below  $\text{pH}_t$ , particle swelling occurs because of ionization of inside groups. In this region, the charge density arises from two distinct contributions: bulk and surface charge.

As a consequence, the expression for the microgel charge density is modelled as

$$\rho_{fix} = \begin{cases} \frac{3\sigma_s(\text{pH})}{r} \delta_{rb} & \text{pH} \leq \text{pH}_t \\ \frac{3\sigma_s(\text{pH})}{r} \delta_{rb} + \rho_{in}(\text{pH}) & \text{pH} > \text{pH}_t \end{cases} \quad (17)$$

where  $\delta_{rb}$  is the Kronecker delta function and  $\rho_{in}$  and  $\sigma_s$  are the volume and surface charge densities, respectively.

The total equilibrium potential may be considered as the sum of two contributions (assuming field superposition), one arising from the surface charge,  $\psi_s^{(0)}$ , and another from the charge inside the microgel,  $\psi_{in}^{(0)}$ . For this particular case equation (15) is rewritten in the following way:

$$G(r) = \frac{\epsilon_0 \epsilon_r \kappa^2}{\eta} \frac{d}{dr} (\psi_{in}^{(0)} + \psi_s^{(0)}). \quad (18)$$

These equilibrium potentials can be analytically calculated by solving the linearized Poisson equation [7, 12]. The introduction of the corresponding expressions into  $G(r)$ , and of this function into the general mobility expression (12), yields the following result:

$$\mu = \begin{cases} \mu_s & \text{pH} \leq \text{pH}_t \\ \mu_s + \mu_{in} & \text{pH} < \text{pH}_t \end{cases}$$

where

$$\mu_s = \frac{\sigma_s}{\eta \lambda^2} \left[ \frac{3}{b} + \frac{8\pi}{b} \left( 1 - \frac{\lambda b}{3} \frac{\sinh(\lambda b)}{\cosh(\lambda b) - [\sinh(\lambda b)]/\lambda b} \right) + \frac{8\pi b \lambda^2}{3(1 + \kappa b)} \right] \quad (19)$$

$$\mu_{in} = \frac{\rho_{in}}{\eta \lambda^2} \left[ 1 + \frac{1}{3} \frac{\lambda^2}{\kappa^2} \left( 1 + e^{-2\kappa b} - \frac{1 - e^{-2\kappa b}}{\kappa b} \right) + \frac{1}{3} \frac{\lambda^2}{\kappa^2} \frac{1 + 1/(\kappa b)}{\lambda^2/\kappa^2 - 1} \left( \frac{\lambda}{\kappa} \frac{1 + e^{-2\kappa b} - (1 - e^{-2\kappa b})/(\kappa b)}{(1 + e^{-2\lambda b})/(1 - e^{-2\lambda b}) - 1/(\lambda b)} - 1 + e^{-2\kappa b} \right) \right]. \quad (20)$$

It is worth emphasizing that the model described is only valid for low potentials. Under these conditions the Poisson equation may be analytically solved to give the electrophoretic mobility equations (19) and (20). As can be seen in this case, the electrophoretic mobility of the microgel particle depends on (i) the internal structure through the friction coefficient and (ii) both the surface and bulk charge densities, in a linear fashion.

## 4. Materials and methods

### 4.1. Particle size and electrophoretic mobility measurements

Photon correlation spectroscopy (PCS) [13] has been employed to determine size of the microgel particles, and hence to monitor the volume transition of the microgel particles as the pH changes.

A Malvern Zetamaster-S, with a diode laser working at a wavelength of 670 nm was employed to measure the intensity autocorrelation function.

The equipment used for obtaining the electrophoretic mobility from the measured autocorrelation function was a Malvern Zetamaster-S working with a He-Ne laser of wavelength 632.8 nm.

All PCS and electrophoretic measurements were done in a dilute regime, in order to avoid interactions between particles and multiple scattering. Particle concentration was optimized to be  $5 \times 10^9 \text{ cm}^{-3}$ . Prior to undertaking the measurements, suspensions were sonicated for about two minutes, even though a detailed study of the influence of this treatment showed no significant size variation with varying time of sonication.

#### 4.2. Experimental system

The microgel used was a cationic poly-(2-vinylpyridine) microgel, crosslinked with divinylbenzene (0.25%). The diameter in the collapsed state was determined by TEM to be  $205 \pm 8$  nm [11]. It is a highly charged system, as established in reference [8], with both surface and interior charge contributions. The microgel dispersion was dialysed against ultra-pure water for a total of 21 days with two changes of water per day in order to remove unreacted materials and low-molecular-weight oligomers [11].

The background electrolyte concentration was 1 mM NaCl for all suspensions. The pH was fixed by the addition of HCl or NaOH. The temperature was set to 25 °C.

### 5. Results and discussion

#### 5.1. Microgel swelling

The swelling transition between the collapsed and swollen states of the microgel particle is associated with a large volume change in the particle. This transition can be induced by variations of different external conditions, such as temperature [15], ionic strength [16] or solvency [17].

The microgel employed in this work contains weak ionizable groups; hence the pH was chosen for triggering the particle swelling. Figure 1 shows the PCS particle diameter as a function of pH. As can be seen, from high pH values down to  $\text{pH} = \text{pH}_i = 4.8$ , the microgel is in its unswollen state (TEM diameter). Below  $\text{pH}_i$ , the hydrodynamic size increases abruptly, as a consequence of the interior group ionization [8]. The correlation between the inner particle charge and its volume has recently been described using the Flory–Huggins theory for gels [8].

Figure 2 is a plot of the volume charge density versus pH. The charge density was calculated

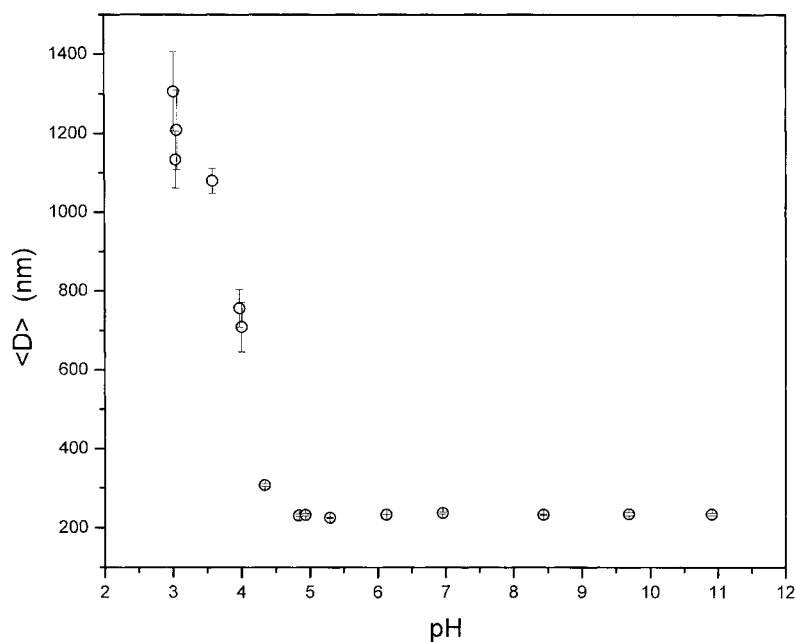
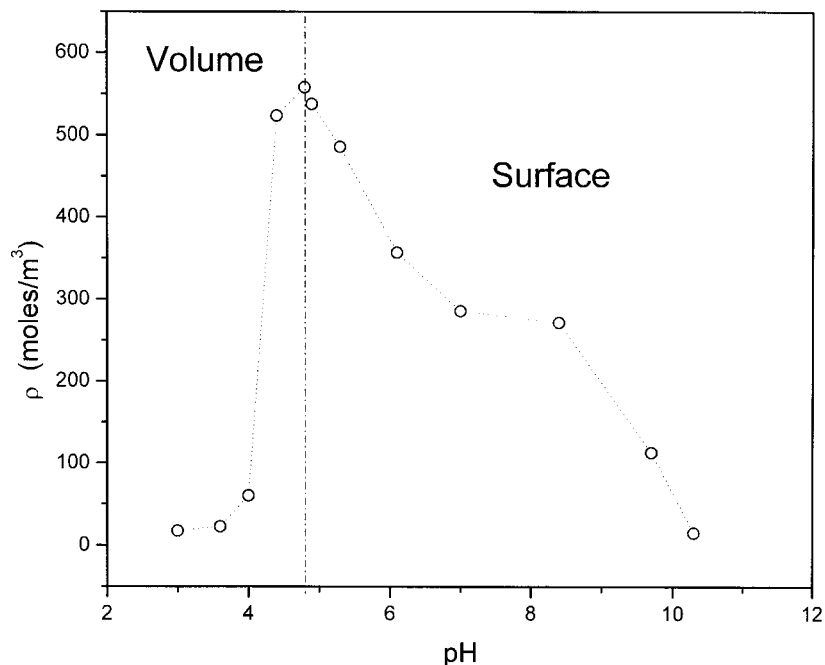


Figure 1. Hydrodynamic diameter as a function of pH.

from figure 1 and charge titration [8]. Above pH 4.8 only the particle surface is charged (see equation (17)). As can be seen, the charge density presents a maximum at pH 4.8, which arises from the increase in particle size below this transition pH. The decrease is very abrupt until pH 4 is reached, while below this pH value, it keeps decreasing at a much lower rate.



**Figure 2.** Particle charge density versus pH. The terms ‘Volume’ and ‘Surface’ refer to the location of the particle charge within the corresponding pH region.

## 5.2. Hydrodynamics

The swelling of the microgel particles is accompanied by internal structure modifications. As the microgel network is symmetric (the applied electric field is weak enough that its effect does not lead to deformation), the friction tensor appearing in equation (2) is actually a scalar: the friction coefficient,  $\gamma$ . The estimation of  $\gamma$  is not easy, neither theoretical nor experimentally. A simple argument for deriving it is sometimes employed in the literature [7]: it considers that each ‘resistive element’ within the particle corresponds to a polymer segment, which in turn is regarded as a sphere of radius  $R$ . The polymer segments are considered to be distributed at a volume density  $N$  within the microgel particle. Each polymer segment will exert a Stokes resistance  $6\pi\eta R\vec{u}$  on the liquid flow through the gel. This reasoning leads to the following equation for  $\gamma$ :

$$\gamma = 6\pi\eta RN. \quad (21)$$

However, it is now well known that the hydrodynamic friction of a polyelectrolyte cannot be calculated as the sum of independent Stokes frictions of segments [18]. Hydrodynamic interactions have to be accounted for.

Brinkman [19, 20] calculated the friction coefficient of a macromolecule by treating it as a spherical cloud of homogeneously distributed beads, obtaining the following expression:

$$\gamma = \eta \frac{72}{R^2} \left\{ 3 + \frac{4}{\phi} - 3 \left( \frac{8}{\phi} - 3 \right)^{0.5} \right\} = \eta \frac{72}{R^2} f(\phi) \quad (22)$$

where  $\phi$  is the polymer volume fraction within the microgel particle. Our experimental electrophoretic mobilities suggest that the function  $f(\phi)$  should decrease faster than predicted by the Brinkman equation, as the polymer volume fraction is lowered. This is required to reduce the friction sufficiently, at high particle swellings, in order to obtain the trend in the theoretical electrophoretic mobility (see the next section). The empirical function  $f(\phi) = \phi/(1 - \phi)$  yields correct behaviours for  $\phi \rightarrow 0$  (swollen state) and  $\phi \rightarrow 1$  (totally collapsed state). This  $\gamma$ -dependence on  $\phi$  has been proposed previously by other authors [9], and is based on empirical arguments (see also [21] and [22]). The microgel size  $b$  is related to the segment length  $R$  by a linear relation,  $b \sim R$  [19], the proportionality constant being related to the number of chains along a diameter of the microgel, especially when the micronetwork is swollen.

The following expression of the friction coefficient is used in this work:

$$\gamma \sim \frac{\eta}{b^2} \frac{\phi}{1 - \phi}. \quad (23)$$

For isotropic swelling the relation between the microgel particle volume  $V$  and polymer volume fraction is given by [14]

$$\frac{\phi}{\phi_0} = \frac{V_0}{V} = \frac{(2b_0)^3}{(2b)^3} \quad (24)$$

where  $V_0$  and  $\phi_0$  refer to a reference state which is taken as  $\phi_0 = 1$  for  $2b_0 = \text{TEM diameter}$ .

Expression (22) for the friction coefficient is developed in the absence of an external electric field (non-electrophoretic conditions) and thus it is strictly valid for low salt concentrations. At high electrolyte concentration, a uniformly charged polyelectrolyte can be considered as 'free draining' since hydrodynamic interactions between chain segments are screened by the counterions [23]. In this work, the experimental counterion concentration under which all measurements have been performed enables the use of equation (22) for the friction coefficient.

### 5.3. Electrokinetic behaviour

The experimental electrophoretic mobility versus pH is shown in figure 3. The mobility increases as the pH is lowered from 11 to 4.8, then decreases until pH 4 is reached and then increases again for pH values lower than 4. Thus, the curve is characterized by the presence of a maximum (at pH 4.8) and a minimum (at pH 4), which are the consequence of the competition between variations in the charge density and in the friction coefficient.

The experimental charge density (figure 2) is superficial above  $\text{pH}_t$  (see equation (17)). The forms of figures 2 and 3 in this region are similar and hence the velocity of the particle seems to be governed by the surface charge-density variation. Between pH 4.8 and pH 4, the charge density, which is now the sum of the surface and volume contributions, decreases abruptly. In this same region the friction coefficient also decreases, implying a reduction in the frictional force. The particle mobility also decreases in this region (figure 3), which seems to indicate that the influence of the charge density dominates over the friction coefficient variations. Finally, below pH 4, the charge density keeps decreasing but at a lower rate, while



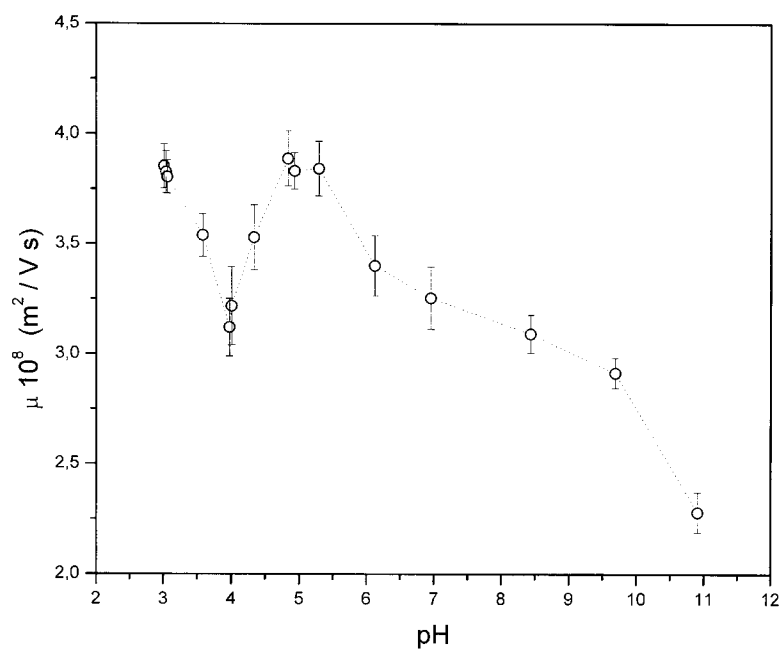


Figure 3. Experimental electrophoretic mobility versus pH.

the particle size increases (figure 1), reducing even more the frictional force between the fluid and the network. Hence, the electrophoretic velocity increases (figure 3) in this region.

In order to test these hypothesis, the experimental charge densities and the expression for  $\gamma$  (equation (23)) have been introduced in the theoretical expression for the electrophoretic mobility (equations (19), (20)) yielding the results shown in figure 4. As may be seen, the

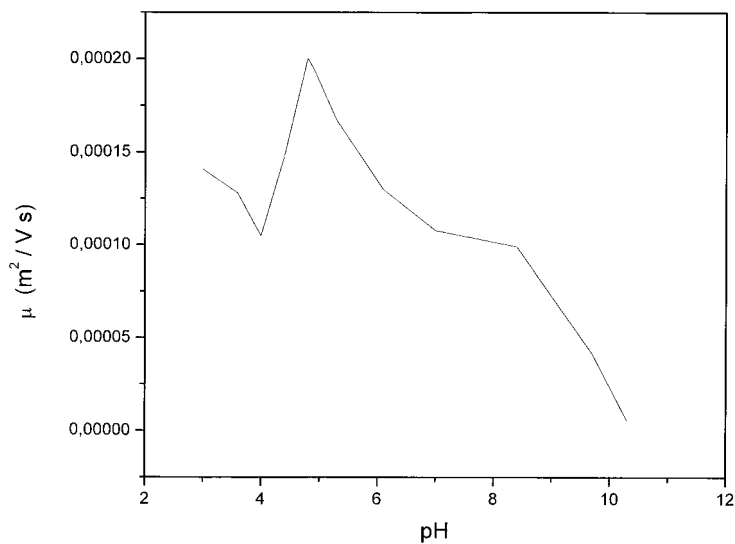


Figure 4. Theoretical electrophoretic mobility as a function of pH.

experimental and theoretical curves have the same approximate, qualitative form. The presence of the maximum and minimum is again observed. However, quantitatively, the theoretical values are much larger than the ones obtained experimentally.

From a strict mathematical point of view, the use of the linearized form of the Poisson equation is probably a gross oversimplification. It is only valid for particle charges yielding low potentials. This condition is not fulfilled in the case of the microgel studied here [8]. The solution to this problem comes by using a renormalization procedure for the charge. The charge densities appearing in expressions (19) and (20) should be regarded as effective charge densities,  $\sigma_s^{eff}$  and  $\rho_{in}^{eff}$ . For dense colloidal systems the procedure proposed by Alexander *et al* [24] seems to give good results when comparing experimental and theoretical results. However, all our experiments were performed in the regime of dilute particle concentration, where interactions between particles do not play a significant role. As a consequence, this physical interpretation for the effective charge is not valid. An alternative physical interpretation of the 'effective charge' is needed. This could be based on ion condensation effects [25–28]. The observed discrepancy between the experimental and theoretical electrophoretic mobility values could then be a measure of this effect.

## 6. Conclusions

The electrophoretic mobility of microgel particles shows a strong sensitivity to changes in charge density and friction coefficient, giving rise to the appearance of a maximum and a minimum in the  $\mu$ -pH curve. The experimental curve may be qualitatively accounted for in terms of the experimental particle charge distribution, but taking into account changes in the hydrodynamic friction forces caused by the particle swelling. Ohshima's general theory for polyelectrolyte-coated particles may then be applied to account for the electrophoretic mobility-pH results. The main discrepancy lies in the quantitative differences between the experimental and theoretical electrophoretic mobilities, pointing to some charge renormalization. One possibility here is ion condensation.

## Acknowledgments

The authors would like to thank Dr Andrew Loxley (University of Bristol) for supplying the microgel particles. This work was supported by the *Acción Integrada Hispano-Británica* HB1998-0225.

## References

- [1] English A E, Tanaka T and Edelman E R 1996 *J. Chem. Phys.* **125** 10 606
- [2] Peppas N A 1997 *Curr. Opin. Colloid Interface Sci.* **2** 531
- [3] Kajiwara K and Rossmurphy S B 1992 *Nature* **355** 208
- [4] Quadrat O and Snupek J 1990 *Prog. Org. Coatings* **18** 207
- [5] Sawai T, Yamazaki S, Ikariyama Y and Aizawa M 1991 *J. Electroanal. Chem.* **297** 297
- [6] Morris G M, Vincent B and Snowden M J 1997 *J. Colloid Interface Sci.* **190** 198
- [7] Ohshima H 1995 *Adv. Colloid Interface Sci.* **62** 189
- [8] Fernández-Nieves A, Fernández-Barbero A, Vincent B and de las Nieves F J 2000 *Macromolecules* at press
- [9] Cohen Stuart M A, Waajen F H W H, Cosgrove T, Vincent B and Crowley T L 1984 *Macromolecules* **17** 1825
- [10] Hunter R J 1995 *Foundations of Colloid Science I* (Oxford: Clarendon)
- [11] Loxley A and Vincent B 1997 *Colloid Polym. Sci.* **275** 1108
- [12] Verwey E J W and Overbeek J Th G 1948 *Theory of the Stability of Lyophobic Colloids* (New York: Elsevier)
- [13] Pecora R 1985 *Dynamic Light Scattering* (New York: Plenum)
- [14] Hirotsu S 1994 *Phase Transitions* **47** 183

- [15] Hirotsu S 1993 *Adv. Polym. Sci.* **110** 1
- [16] Riäka J and Tanaka T 1984 *Macromolecules* **17** 2916
- [17] Tanaka T 1978 *Phys. Rev. Lett.* **40** 820
- [18] Kirkwood J G and Riseman J 1948 *J. Chem. Phys.* **16** 565
- [19] Brinkman H C 1947 *Proc. Acad. Sci., Amsterdam* **50** 618
- [20] Brinkman H C 1949 *Research* **2** 190
- [21] Mijnlieff P F and Jaspers W J 1971 *Trans. Faraday Soc.* **67** 1837
- [22] Vidakovic P, Allain C and Rondelez F 1982 *Macromolecules* **15** 1571
- [23] Long D, Viovy J-L and Ajdari A 1996 *Phys. Rev. Lett.* **76** 3858
- [24] Alexander S, Chaikin P M, Grant P, Morales G J, Pincus P and Hone D 1984 *J. Chem. Phys.* **80** 5776
- [25] Manning G S 1978 *Q. Rev. Biophys.* **2** 179
- [26] Tamashiro M N, Levin Y and Barbosa M C 1998 *Physica A* **258** 341
- [27] Levin Y, Barbosa M C and Tamashiro M N 1998 *Europhys. Lett.* **41** 123
- [28] Fernández-Nieves A, Fernández-Barbero A and de las Nieves F J 2000 *Langmuir* at press